Transactions of the SMiRT 27
Yokohama, Japan, March 3-8, 2024
Division IV

ESTIMATION OF STRONG MOTION GENERATION AREAS OF LARGE EARTHQUAKES USING A HYBRID HEURISTIC METHOD

Naoya Ishikawa[1], Satoshi Iwase[2], Kentaro Motoki[3], Hiroaki Kobayashi[4], and Koichi Yabuuchi[5]

[1] Manager, Chubu Electric Power Co., Inc., Aichi, Japan (Ishikawa.Naoya@chuden.co.jp)
[2] Senior Manager, Chubu Electric Power Co., Inc., Aichi, Japan
[3] General Manager, Kobori Research Complex, Inc., Tokyo, Japan
[4] Deputy Manager, Kobori Research Complex, Inc., Tokyo, Japan
[5] Group Leader, Kajima Corporation, Tokyo, Japan

ABSTRACT

We performed strong motion generation area (SMGA) inversions, using a hybrid heuristic method, merging genetic algorithms and simulated annealing, for the 2003 Tokachi-oki and the 2005 Miyagi-oki earthquakes, Japan to validate this inversion scheme. The locations of inverted SMGAs were consistent with those reported in previous studies. This method objectively estimates the SMGAs for huge earthquakes. Our future work will involve conducting SMGA inversions for numerous subduction earthquakes to explore SMGA characteristics such as the depth dependence of the stress drop.

INTRODUCTION

In Japan, the design of a nuclear power plant requires consideration of the design basis ground motions. These are determined by evaluating two types of ground motions: “site-specific ground motions evaluated by specifying seismic sources” and “ground motions evaluated without specifying seismic sources” (Wu et al., 2018). For the former evaluation, source models were constructed using the strong ground-motion prediction method “Recipe” (Irikura, 2004). In the recipe, the source model is composed of a characterized source model involving asperities and background areas (Somerville et al., 1999).

Asperities, characterized by a substantial slip relative to the average slip on a fault, substantially influence the predicted ground motion. Their parameters are crucial, especially considering that asperities typically align with strong motion generation areas (SMGAs; Miyake et al., 2003). Precise estimation of SMGA parameters is vital for accurate ground-motion prediction. While each SMGA involves numerous parameters, they are frequently determined through forward modeling or a grid search approach, often resulting in a limited number of parameters being determined. Consequently, a more objective method for determining the SMGA parameters is desired.

In this study, we applied a hybrid heuristic method that combines a genetic algorithm and simulated annealing (Yamanaka, 2007) to determine SMGA parameters. To investigate the method’s performance, we analyzed the 2003 Tokachi-oki and 2005 Miyagi-oki earthquakes and compared inverted SMGA models with SMGA models from previous studies.

METHOD

We adopted the empirical Green’s function (EGF) method to synthesize the ground motions of a large earthquake from the observed ground motions of a small earthquake. The EGF method assumes that the observed ground motions of a small earthquake were close to Green’s functions and superimposes them to match the scaling law between small and large earthquakes. The observed ground motions of the small earthquake are superimposed in the fault length direction (N_L), width direction (N_W), and slip time direction (N_D). Here, we set $N_L = N_W = N_D = N$. The formulae used to synthesize the waveforms are as follows:

$$\mathrm{U}(t) = \sum_{i=1}^{N}\sum_{j=1}^{N}\frac{r_{elm}}{r_{ij}}F(t) * \left(C \cdot u\left(t - t_{ij}\right)\right), \tag{1}$$

$$\mathrm{F}(t) = \delta(t) + \frac{1}{n'\left(1-\frac{1}{e}\right)}\sum_{k=1}^{(N-1)n'}\frac{1}{e^{\frac{(k-1)}{(N-1)n'}}}\left[\delta\left\{t - \frac{(k-1)T}{(N-1)n'}\right\}\right], \tag{2}$$

$$t_{ij} = \frac{r_{ij} - r_{elm}}{Vs} + tr_{ij}, \tag{3}$$

$$tr_{ij} = t_{start} + \frac{\xi_{ij}}{Vr} + \varepsilon, \tag{4}$$

where, U(t) and u(t) are the displacements during a large earthquake and a small earthquake, r_{elm}, r_{ij} and ξ_{ij} are the hypocentral distance of the small earthquake, the distances between the station and the ith and jth elements in SMGA, respectively, a distance between two rupture trigger points from the ith to jth elements, C is the stress drop ratio of the SMGA to the small earthquake, N is the number to superimpose, F(t) is a filter function, δ is Dirac's delta, T is the rise time of the SMGA, Vs is the S-wave velocity at the seismogenic layer, and ε is the fluctuation of rupture time. n' is the number to be adjusted so that artificial contaminations do not appear when superimposing, and * means convolution. To avoid a fall-off in the intermediate frequency during synthesis, a source time function close to the Kostrov type was used based on the Irikura method (Miyake et al., 2003). In addition, although the above formulation uses convolution in the time domain, because many waveforms need to be synthesized in the inversion, convolution was performed in the frequency domain to increase the computational performance.

We used a hybrid heuristic method (Yamanaka, 2007), which combines the genetic algorithm and the simulated annealing, for the SMGA inversion using the EGF method. This method does not require the setting initial values, and can objectively determine the parameters of the SMGAs. The following formula gives the error function, Misfit, used in this study:

$$\mathrm{Misfit} = \frac{1}{\mathrm{N_{obs}}}\sum_{i=1}^{\mathrm{N_{obs}}}\mathrm{Misfit}_i, \tag{5}$$

where, Misfit_i is the error at the ith station and N_{obs} is the number of stations. The error at each station is calculated using the following formula: the summation of the L2 norm of the Fourier amplitude residual and the envelope residual of the acceleration waveforms. The standard deviation σ in the Fourier amplitude was assumed to be the aleatory variability and was set to 0.4, referring to Hikita et al. (2018).

$$\mathrm{Misfit}_i = \mathrm{p} \cdot \frac{1}{\mathrm{N_{comp}}}\sum_{j=1}^{\mathrm{N_{comp}}}\frac{\sum_t\left(eobs_{i,j}(t) - ecal_{i,j}(t)\right)^2}{\sqrt{\sum_t\left(eobs_{i,j}\right)^2\sum_t\left(ecal_{i,j}\right)^2}}$$
$$+(1-p) \cdot \frac{1}{\mathrm{N_{comp}}}\sum_{j=1}^{\mathrm{N_{comp}}}\frac{\log\left\{\sum_f\left(Fobs_{i,j}(f)\right)/\sum_f\left(Fcal_{i,j}(f)\right)\right\}^2}{\sigma^2}, \tag{6}$$

where i and j indicate the ith station and jth component, $eobs_{i,j}$ and $ecal_{i,j}$ are the envelope of observed and calculated acceleration, and $Fobs_{i,j}$ and $Fcal_{i,j}$ are the Fourier amplitude of observed and calculated acceleration. The p is the weight on the acceleration envelope applied in the inversion, and was set to 0.5 in this study.

In the hybrid heuristic method, we set the number of populations to 200, and the maximum number of generations was determined through trial and error while checking the analysis results. For mutation, the function of Michalewicz (1992) was used. In this study, calculations were performed in 10 trials with different random numbers, and the model with the minimum Misfit among the 10 trials was considered as the final result.

DATA AND CONDITIONS FOR INVERSION

The primary aim of this study is to validate the inversion analysis of SMGAs. To achieve this, we selected data and conditions for inversion, such as an element earthquake, stations, and fault geometry to align with those used in previous studies. The inverted results were subsequently compared with the results from the corresponding studies. Specifically, we replicated the data and conditions used by Kamae and Kawabe (2004) for the 2003 Tokachi-oki earthquake and Kamae (2006) for the 2005 Miyagi-oki earthquake. Figure 1 illustrates the station used in the analysis and the epicenters of the element earthquakes. We used the ground motions obtained at the down-hole of KiK-net. The nonlinear effects of subsurface geology were omitted from consideration because they were negligible in both of acceleration envelopes and Fourier amplitudes, even during the main shock.

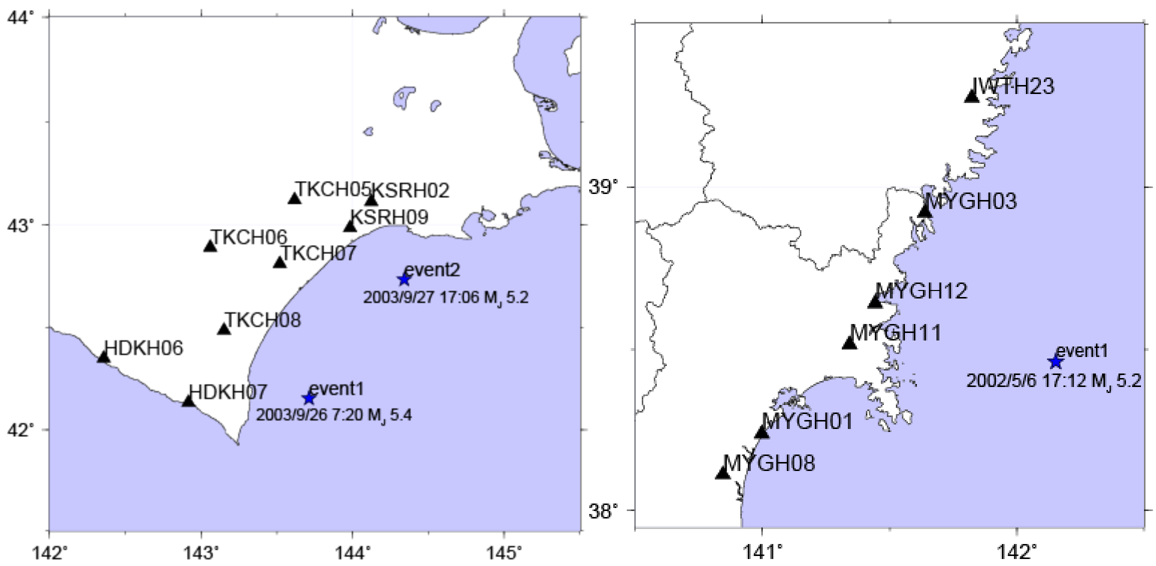

Figure 1. Map showing the KiK-net stations (triangles) used in the inversion and epicenters of the element earthquakes (stars) used as the empirical Green's function.

The parameters under investigation encompassed the SMGA position, the initiation point of the rupture within the SMGA (identifying the element that initiates rupture), superposition number, stress drop ratio, random number controlling the fluctuation of the rupture front, and average rupture velocity within the SMGA. Table 1 illustrates the search ranges for these parameters. The fault range was determined based on pertinent previous studies, and the search ranges for all the parameters were established to encompass the results for comparison. In this study, Brune's formula (Brune, 1970, 1971) was employed to delineate the relationship between the corner frequency (fc) and area (S) of an element earthquake.

We started the inversion process with a single SMGA, and incrementally added the SMGAs. We narrowed the search area to SMGAs inverted in its iterative process. The objective function comprised both the Fourier amplitude and acceleration envelope. Fourier amplitude calculations used data spanning 163.84 seconds and acceleration envelope used 60 seconds from 3 seconds before the arrival of the S-wave, considering the rupture duration of the main shock. The maximum number of generations was set to 4000 for one SMGA, 7000 for two SMGAs, and 10000 for three SMGAs. In addition, the total seismic moment (M_0) of the SMGAs was constrained to not exceed the value of Global CMT. For the 2005 Miyagi-oki earthquake, we considered up to two SMGAs as estimated by Kamae (2006). For the Tokachi-oki Earthquake, we explored a scenario with three SMGAs, as estimated by Kamae and Kawabe (2004). However, there was a minimal difference in Misfit, synthetic waveforms, and response spectra between the two and three SMGAs. Therefore, we adopted two SMGAs for the final results.

Table 1: Search ranges of unknown parameters of SMGAs in the 2003 Tokachi-oki and the 2005 Miyagi-oki earthquakes.

unknown parametes	the 2003 Tokachi-oki earthquake	the 2005 Miyagi-oki earthquake
the location of SMGA along strike direction (km)	-75 ~ -45	0 ~ 48
the location of SMGA along dip direction (km)	-5 ~ -75	0 ~ 74
the rupture starting point (which element begin to rupture)	1 ~ N	1 ~ N
the average Vr before SMGA rupturing (km/s)	2.2 ~ 3.8	2.7 ~ 3.9
rise time (s)	0.5 ~ 4.0	0.2 ~ 1.0
Vr within SMGAs (km/s)	2.4 ~ 3.8	2.7 ~ 3.9
random number to control the fluctuation of rupture front	five kind of numbers	five kind of numbers
the stress drop ratio C	0.2 ~ 20	0.2 ~ 50
the superposition number N	3 ~ 9	2 ~ 6

RESULTS

The values of the unknown parameters in 10 solutions were relatively stable. This highlights the suitability of the inversion scheme for SMGA inversion. For example, for the results of the 2005 Miyagi-oki earthquake, a comparison of waveforms between observed and calculated with the inverted model is shown in Figure 2, and the response spectra are shown in Figure 3. Although inversion was performed to match the acceleration envelope, it was confirmed that not only the acceleration but also the velocity and displacement waveforms were generally reproduced. The reproducibility of the response spectra was higher than that in previous studies. The reproducibility of the waveforms and response spectra was also confirmed for the 2003 Tokachi-oki earthquake.

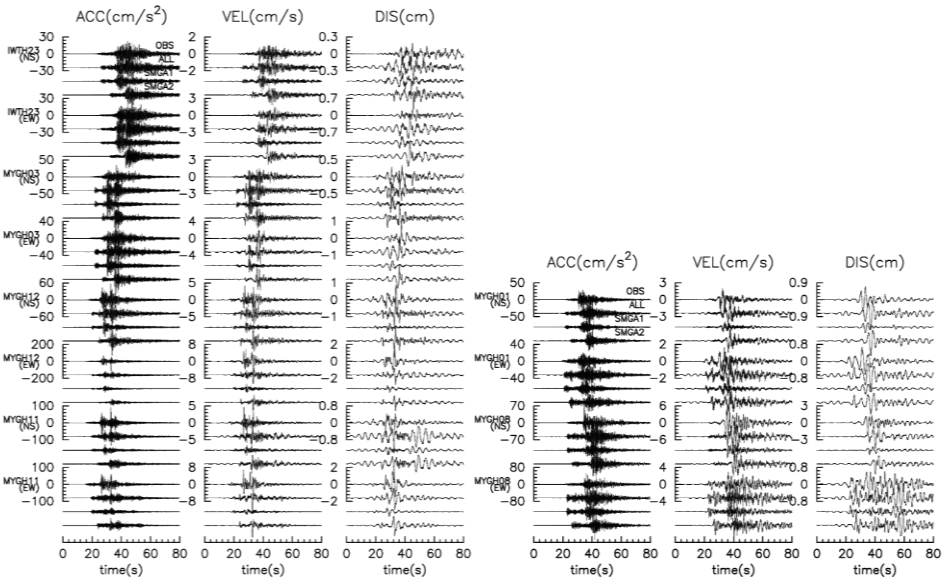

Figure 2. Comparison of the synthesized waveforms from all SMGAs and from each SMGA with the observed waveforms for the 2005 Miyagi-oki earthquake.

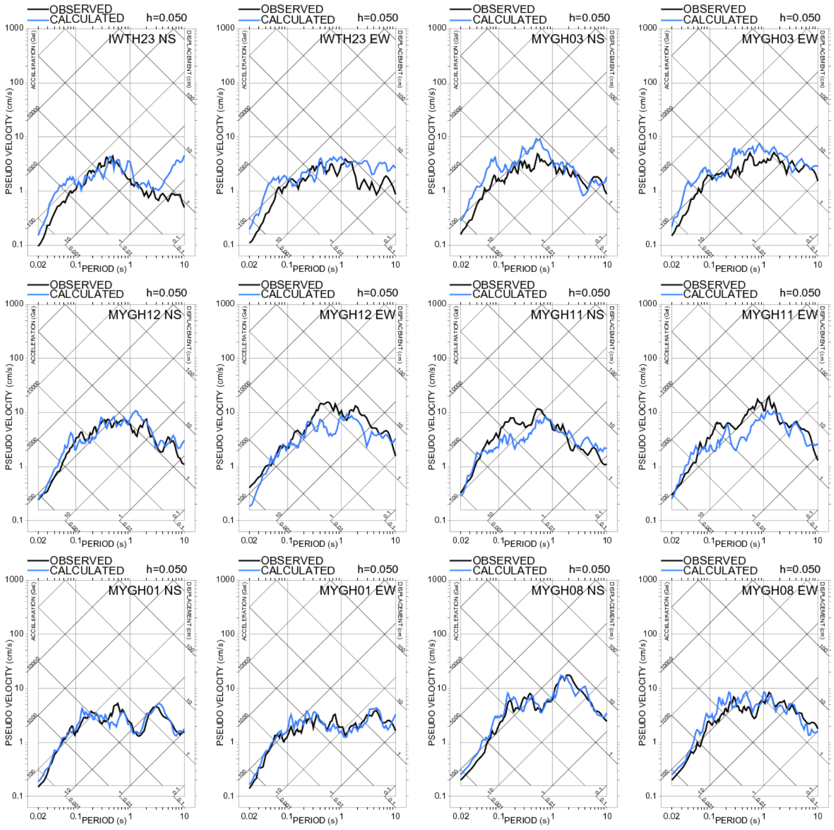

Figure 3. Comparison of the pseudo response spectra of the synthesized motions (with blue lines) from all SMGAs with those of the observed records (with black lines) for the 2005 Miyagi-oki earthquake.

DISCUSSION

Figures 4 and 5 illustrate a comparison of the SMGA locations between the inverted model and the model estimated in previous studies. The 2005 Miyagi-oki earthquake aligned well with the SMGA locations identified by Kamae (2006). Regarding the 2003 Tokachi-oki earthquake, the SMGAs in the inverted model closely resembled the shallow SMGA (Asp 1) and western SMGA (Asp 2) identified by Kamae and Kawabe (2004). However, the inversion method did not resolve Asp 3, the smallest of the three SMGAs. Kamae and Kawabe (2004) focused on reproducing the pulses observed in the velocity waveforms of TKCH07, HDKH07, and KSRH02 and determined Asp3 based on the waveform of KSRH02. In contrast, this study employed the acceleration envelope and Fourier amplitude as objective functions and the inverted model effectively reproduced the acceleration envelope and pseudo-velocity response spectra of KSRH02. One potential explanation for the non-estimation of Asp3 was the difference in the objective functions employed.

Comparing the SMGA parameters, the stress drop is smaller than that of Kamae and Kawabe (2004) Asp1 for the 2003 Tokachi-oki earthquake. The SMGA area surpassed that in previous study, and the entire SMGA moment was also large. When comparing Asp1 and Asp2 of the 2003 Tokachi-oki earthquake, the area and overall moment exceeded those in the previous study. The previous research indicated that Asp3 contributes 18-25% of the entire SMGA moment, 8-21% of the area, and 4-37% of the short-period level. In addition, in Kamae and Kawabe's (2004) model, some stations exhibited underestimated pseudo velocity response spectra in the long period range. However, in this study's model, except for the EW component of KSRH09, the observed spectra were successfully reproduced even in the long period range. The estimated value aligns closely with the previous studies at the total short-period level. The larger area of the inverted SMGA compared to the previous studies might be attributed to this method attempting to adjust the entire ground motion using only SMGA, whereas previous studies aimed to reproduce the pulse-like waves.

the inverted model	Kamae (2006)
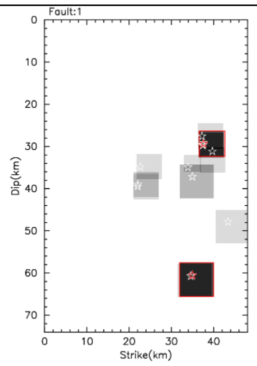	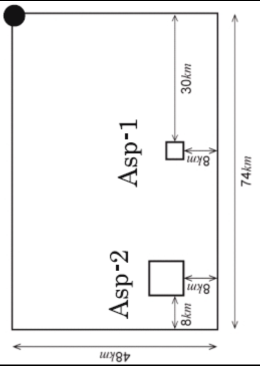

Figure 4. Comparison of the SMGA locations between Kamae (2006) and the inverted model for the 2003 Miyagi-oki earthquake. In the inverted model, each solution with 10 times random number is shown with light gray rectangular and the dark gray means overlaid many solutions, and the best solution with the red one.

the inverted model	Kamae and Kawabe (2004)
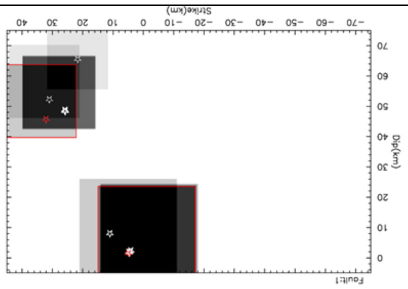	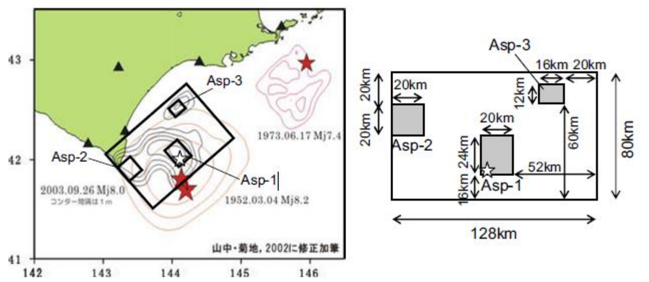

Figure 5. Comparison of the SMGA locations between Kamae and Kawabe (2004) and the inverted model for the 2003 Tokahi-oki earthquake. In the inverted model, each solution with 10 times random number is shown with light gray rectangular and the dark gray means overlaid many solutions, and the best solution with the red one. The entire fault plane in inverted model is almost the same as Kamae and Kawabe (2004), and the directions are aligned.

Table 2: Comparison of SMGA parameters of between this study and the previous study for the 2005 Miyagi-oki earthquake.

parameter	unit	Deep SMGA		Shallow SMGA	
		this study	Kamae (2006)	this study	Kamae (2006)
rise time	s	0.4	0.6	0.6	0.4
the ratio of stress drop over element earthquake		6.38	10	8.58	30
rupture velocity in SMGAs	km/s	3.3	3.1	3.5	3.1
the superposition number		4	4	3	2
area	km^2	64	64	36	16
seismic moment	Nm	4.08E+18	6.39E+18	2.31E+18	2.40E+18
short-period level (the flat level of an acceleration source spectra)	Nm/s^2	1.70E+19	2.66E+19	1.71E+19	4.00E+19
stress drop	MPa	19.1	30	25.7	90

Table 3: Comparison of SMGA parameters of between this study and the previous study for the 2003 Tokachi-oki earthquake. SMGA3 was not reproduced by the inversion.

parameter	unit	Deep SMGA		Shallow SMGA		SMGA3
		this study	Kamae and Kawabe (2004)	this study	Kamae and Kawabe (2004)	Kamae and Kawabe (2004)
rise time	s	2	-	1.5	-	-
the ratio of stress drop over that of the element earthquake		6.99	10	6.76	5	5
rupture velocity in SMGAs	km/s	3.4	2.8	3.4	2.8	2.8
the superposition number		8	5, 6, 5.5	6	5, 5, 5	4, 3, 3.5
area	km^2	1024	480	576	400	192
seismic moment	Nm	5.01E+20	2.31E+20	1.49E+20	8.75E+19	2.94E+19
short-period level (the flat level of an acceleration source spectra)	Nm/s^2	1.23E+20	1.19E+20	6.48E+19	5.43E+19	3.76E+19
stress drop	MPa	35	50	33.8	25	25

As previously mentioned, the SMGA identified in this study exhibited a larger area and smaller stress drop than the SMGA estimated by forward modeling in the previous studies. One reason for this difference is the objective function used. This study's objective function comprises the Fourier amplitude and acceleration envelope, whereas the previous studies focused on the pulse-like waves. In the SMGA inversion, it is assumed that SMGAs reproduce all the strong ground motions in both short and long period ranges. However, in the long-period range, the background region, which was ignored in the SMGA inversion, can contribute to some extent. In such cases, the total moment of the SMGA becomes high, the "N" of the SMGA becomes large and consequently the area of the SMGA becomes large. Because the total short-period level "A" is fixed to evaluate the ground motions, this can decrease the amount of stress drop. Considering the background region or limiting the frequency range of the Fourier amplitude used for the objective function may offer potential solutions to these problems.

Given that this method assesses SMGAs using objective rather than subjective judgment, it offers the potential to provide objective information when analyzing numerous earthquakes. However, it is crucial to acknowledge that, as the method employs the EGF approach, the parameters of the SMGAs are derived as a ratio of element earthquakes. It is important to note that the final results may vary depending on the selection of element earthquakes.

CONCLUSION

We developed a method for the SMGA inversion analysis and applied it to the 2003 Tokachi-oki and the 2005 Miyagi-oki earthquakes. The locations of the resulting SMGAs were generally aligned with those estimated by forward modeling in the previous studies. However, one SMGA (the smallest of the three) could not be estimated for the 2003 Tokachi-oki earthquake. Nevertheless, even with the two SMGAs, the waveforms and response spectra were well-reproduced well. When comparing the parameters of the SMGAs in the obtained models with those in the previous studies, there was a tendency for the area to be larger and the stress drop to be smaller. This discrepancy is likely attributable to the differences in the objective function between the present study and the previous studies.

In future studies, we will accumulate information on SMGAs by applying the proposed SMGA inversion method, to a broader range of earthquakes. In addition, we plan to investigate the SMGA characteristics, such as the depth dependence of the stress drop.

REFERENCES

Brune, J. N. (1970). "Tectonic stress and the spectra of seismic shear waves from earthquakes," *J. Geophys. Res.*, 75(26), 4997-5009.

Brune, J. N. (1971). "Correction [to "Tectonic stress and the spectra, of seismic shear waves from earthquakes"]," *J. Geophys. Res.*, 76(20), 5002-5002.

Hikita, T., Koketsu, K., and Miyake, H. (2018). Aleatory variability of observed ground motion amplitude, *J. Jpn Assoc. Earthquake Eng.*, 2_15-2_34.

Irikura, K. (2004). Recipe for predicting strong ground motion from future large earthquake, Annuals of disas, prev. *Inst., Kyoto Univ., 47a*.

Kamae, K. (2006). "Source modeling of the 2005 off-shore Miyagi prefecture, Japan, earthquake (MJMA=7.2) using the empirical Green's function method," *Earth, Planets Space*, 58(12), 1561-1566.

Kamae, K. and Kawabe, H. (2004). "Source model composed of asperities for the 2003 Tokachi-oki, Japan, earthquake (MJMA = 8.0) estimated by the empirical Green's function method," *Earth, Planets Space*, 56(3), 323-327.

Michalewicz, Z. (1992). *Genetic algorithms + data structure = evolution programs*. Springer Verlag.

Miyake, H., Iwata, T., and Irikura, K. (2003). "Source characterization for broadband ground-motion simulation: Kinematic heterogeneous source model and strong motion generation area," *Bull. Seismol. Soc. Am.*, 93(6), 2531–2545.

Someville, P., Irikura, K., Graves, R., Sawada, S., Wald, D., Abrahamson, N., Iwasaki, Y., Kagawa, T., Smith, N., and Kowada, A. (1999). "Characteristics crustal earthquake slip models for the prediction of strong ground motion," *Seismol. Res. Lett.*, 70(1), 59-80.

Wu, C., Kobayashi, G., and Sugaya, K. (2018). *Development of method for seismic ground motion evaluation, RREP-2018-4002*.

Yamanaka, H. (2007). "Inversion of surface-wave phase velocity using hybrid heuristic search method," *BUTSURI-TANSA*, 60(3), 265-275.